International Journal of Greenhouse Gas Control 38 (2015) 80–92

International Journal of Greenhouse Gas Control

journal homepage: www.elsevier.com/locate/ijggc

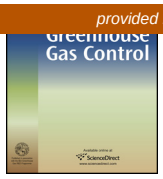

Effect of a controlled sub-seabed release of CO_2 on the biogeochemistry of shallow marine sediments, their pore waters, and the overlying water column

Anna Lichtschlag[a,*], Rachael H. James[a,1], Henrik Stahl[b], Doug Connelly[a]

[a] National Oceanography Centre, University of Southampton Waterfront Campus, European Way, Southampton SO14 3ZH, UK
[b] Scottish Association for Marine Science, Scottish Marine Institute, Oban PA37 1QA, Argyll, UK

ARTICLE INFO

Article history:
Available online 7 November 2014

Keywords:
Carbon capture and storage
CO_2 leakage
Sediment biogeochemistry
Release of metals
Environmental impact

ABSTRACT

The potential for leakage of CO_2 from a storage reservoir into the overlying marine sediments and into the water column and the impacts on benthic ecosystems are major challenges associated with carbon capture and storage (CCS) in subseafloor reservoirs. We have conducted a field-scale controlled CO_2 release experiment in shallow, unconsolidated marine sediments, and documented the changes to the chemical composition of the sediments, their pore waters and overlying water column before, during and up to 1 year after the 37-day long CO_2 release. Increased levels of dissolved inorganic carbon (DIC) were detected in the pore waters close to the sediment-seawater interface in sediments sampled closest to the subsurface injection point within 5 weeks of the start of the CO_2 release. Highest DIC concentrations (28.8 mmol L^{-1}, compared to background levels of 2.4 mmol L^{-1}) were observed 6 days after the injection had stopped. The high DIC pore waters have high total alkalinity, and low $\delta^{13}C_{DIC}$ values (−20‰, compared to a background value of −2‰), due to the dissolution of the injected CO_2 ($\delta^{13}C = -26.6$‰). The high DIC pore waters have enhanced concentrations of metals (including Ca, Fe, Mn) and dissolved silicon, relative to non-DIC enriched pore waters, indicating that dissolution of injected CO_2 promotes dissolution of carbonate and silicate minerals. However, in this experiment, the pore water metal concentrations did not exceed levels considered to be harmful to the environment. The spatial extent of the impact of the injected CO_2 in the sediments and pore waters was restricted to an area within 25 m of the injection point, and no impact was observed in the overlying water column. Concentrations of all pore water constituents returned to background values within 18 days after the CO_2 injection was stopped.

1. Introduction

The greenhouse gas CO_2 is emitted in large quantities from fossil-fuel power plants and other industrial activities, such as the production of concrete and steel. Capture of this CO_2 and its storage in deep geological formations (carbon capture and storage—CCS) is an important technology for reducing global carbon emissions and consequently for contributing to the deceleration of global warming (Energy Technology Perspectives, IEA, 2008; IPCC special report on Carbon Dioxide Capture and Storage, 2005). Large-scale storage of CO_2 is proposed both onshore and off-shore, in deep saline aquifers (Bachu and Adams, 2003; Gunter et al., 1998; Vangkilde-Pedersen et al., 2009), hydrocarbon fields (Kovscek, 2002; Zhang et al., 2011) and un-minable coal seams (Kronimus et al., 2008; White et al., 2005). Within Europe about 40% of the known storage capacity lies offshore, mainly in the North Sea basin (Implementation of Directive 2009/31/EC on the Geological Storage of Carbon Dioxide, 2011). Storage in sub-seabed depleted oil and gas fields is relatively low-risk and cost-efficient compared to other storage options, allowing the removal of large volumes of CO_2 into well sealed reservoirs (Glover, 2009; Holloway, 2005). Nevertheless, potential leakage scenarios include pipeline- and injection failures, failure of the cap rock seal, or leakage through natural fault systems (Bachu and Watson, 2009; Blackford et al., 2009; Burnside et al., 2013; Duncan and Wang, 2014; Gherardi et al., 2007). To ensure the protection of human health and the environment in the event of CO_2 leakage, a number of regulatory frameworks have been put in place (*IPCC Guidelines for National Greenhouse Gas Inventories, 2006; OSPAR Guidelines for Risk Assessment and*

* Corresponding author. Tel.: +44 0 23 8059 6263.
E-mail address: alic@noc.ac.uk (A. Lichtschlag).
[1] Present address: Ocean and Earth Science, National Oceanography Centre, University of Southampton Waterfront Campus, European Way, Southampton SO14 3ZH, UK.

http://dx.doi.org/10.1016/j.ijggc.2014.10.008

Management of Storage of CO_2 Streams in Geological Formations, 2007), which include plans for risk management (*Implementation of Directive 2009/31/EC on the Geological Storage of Carbon Dioxide*). Nevertheless, the potential impacts of CO_2 leakage on the marine environment, and methods for the detection of leakage and its footprint in offshore settings, are at present largely unknown.

At water depths of less than ~300 m, CO_2 released from subseabed storage reservoirs that reaches the surface sediments will either be in the gas phase, or dissolved in the sediment pore waters, which lowers their pH (Eq. (1)):

$$CO_{2(g)} + H_2O_{(l)} \leftrightarrow H_2CO_{3(aq)} \leftrightarrow H^+_{(aq)} + HCO_3^-{}_{(aq)} \leftrightarrow 2H^+_{(aq)} + CO_3^{2-}{}_{(aq)} \quad (1)$$

Laboratory experiments and field studies at natural CO_2 seeps indicate that low-pH fluids can affect benthic ecosystems in a number of ways, including the inhibition of shell formation in some calcifying organisms, reduced metabolic activity and major changes to the composition of bacterial and faunal communities (e.g. Bednarsek et al., 2012; Fabricius et al., 2011; Krause et al., 2012; Murray et al., 2013; Riebesell et al., 2007). In addition, rates of some natural mineral weathering reactions increase at low pH (Ganor et al., 1995), and dissolution and/or desorption of metals from minerals may be enhanced (Payán et al., 2012; Wunsch et al., 2014, 2013). These mobilised metals may accumulate in marine organisms (López et al., 2010), can inhibit growth (De Orte et al., 2014) or even have lethal effects (Riba et al., 2003; Basallote et al., 2014).

While laboratory experiments and studies of natural CO_2 seeps are useful, they cannot fully assess the effects of increased CO_2 concentrations on the benthic ecosystem, either because the ecosystems will have adapted to CO_2 seepage (natural seeps), or because the influences of for instance, the natural seasonal cycling or of biota, cannot be reproduced (laboratory experiments). To test the effects of CO_2 leakage from a CCS reservoir on the marine environment under natural conditions, we therefore conducted a field-scale, in situ CO_2 release experiment in a Scottish sea loch. The experiment, "Quantifying and Monitoring Potential Ecosystem Impacts of Geological Carbon Storage (QICS)", involved the release of 4.2 t of CO_2 at 11 m sediment depth into coastal sediments over a time period of 37 days. Here, we report the results of analyses of the chemical composition of (i) the marine sediments, (ii) their pore waters, and (iii) the overlying water column, before, during and after the CO_2 release. Our data indicate that while the chemical composition of the sediments and the overlying water column were largely unaffected by the release of CO_2, there were significant changes to the composition of the pore waters in the sediments above the injection point. The consequences of these changes for the benthic ecosystem and the recovery of the system are subsequently discussed.

2. Sampling and methodologies

2.1. The QICS experiment

Full details of the QICS experiment can be found in Taylor et al. (2015-b). Briefly, CO_2 gas was released from a borehole drilled through the bedrock, into the upper overlying unconsolidated marine sediments, 350 m offshore in Ardmucknish Bay, on the west coast of Scotland (Fig. 1A). The water depth was 10–12 m, depending on the state of the tide, and the sediments above the injection point were 11 m thick. A total of 4.2 t of CO_2 gas was injected over a time period of 37 days, taking place from May 17th to June 22th 2012.

Within hours of the start of the CO_2 injection, bubbles were observed flowing from the seabed into the water column, and a series of pockmarks formed approximately 2 to 10 m south–west of the CO_2 injection point (Blackford et al., 2014). Seismic imaging showed the presence of a subsurface plume of gas approximately 50 m in diameter 12 days after the start of the CO_2 injection; by the end of the injection the plume was more spatially focussed with a diameter of approximately 20 m (Cevatoglu et al., 2015; Blackford et al., 2014). The bubble streams ceased as soon as the CO_2 injection was stopped (Kita et al., 2015).

To determine the impact and footprint of the injected CO_2 on the near-surface sediments and pore waters, a series of sediment cores, ~20–25 cm long, were collected from: (1) Directly above the CO_2 injection point (Zone 1); (2) 25 m away from the injection point (Zone 2); (3) 75 m away from the injection point (Zone 3); and (4) 450 m away from the injection point (Zone 4) (Fig. 1B). Based on the hydrodynamics of Ardmucknish Bay, Zones 1–3 are influenced by sea water that is potentially affected by the injected CO_2, whereas Zone 4 is a reference site that is unlikely to be affected by the injected CO_2 (Taylor et al., accepted, this issue). Samples of the overlying water column were also taken from all 4 zones. Both sediment and water samples were taken pre-injection (D-7/D-6, i.e. 7 and 6 days before the start of the CO_2 injection), during the gas injection (D13/D14, D34/D35, in May/June 2012), and during 4 sampling campaigns conducted up to 1 year post-injection (D41/D42, D53/D54, D125/D126, D356/D357/D358). Note that 'D' indicates the number of days pre- or post- the start of the CO_2-injection (Table 1).

2.2. Sample collection

Three sediment cores were collected in perspex tubes (5 cm inner diameter) from each zone and on each sampling campaign by Scuba diving and immediately transferred for processing to a temperature controlled room set to the in situ temperature (usually ~10 °C). One core was sub-sampled for solid phase sediment analyses and the remaining two cores were used for sediment pore water extraction. For solid phase analysis, the sediment cores were sliced at 2 cm depth intervals. A sub-sample (3 mL) of each section was transferred into a glass headspace vial containing 5 mL of 1 mol L^{-1} sodium hydroxide and crimp-sealed for methane analysis. Sub-samples for porosity and grain size were stored in pre-weighed plastic containers at 4 °C and the remainder of the sediment sample was freeze-dried for XRF analysis.

Pore waters were extracted from the sediments through predrilled holes in the core liners using Rhizons (*type: CSS, Rhizosphere Research Products, pore size <0.2 μm*), at 2 cm depth intervals in a nitrogen-filled glove bag. Sub-samples of the pore waters were fixed with mercuric chloride in gas-tight glass vials (with no headspace) for dissolved inorganic carbon (DIC) and $\delta^{13}C_{DIC}$ analysis, acidified with 5 μL of thermally distilled (TD) HNO_3 for cation analyses, frozen for nutrient analyses or fixed with zinc acetate for analyses of sulphide and anions. Further sub-samples were taken for the analysis of total alkalinity (TA) immediately after sampling.

Water samples were collected from onboard the research vessel *Seòl Mara* using a 5 L Niskin bottle. Water samples were taken from 5 depths, ranging from 2 m below the sea surface to 1 m above the seafloor, with the absolute depth depending on the tidal range. Sub-samples were transferred into gas tight glass vials without headspace for DIC, TA and dissolved oxygen analyses. Additional sub-samples were frozen in plastic bottles for nutrient analyses. At each sampling site and time point, profiles of conductivity, temperature and depth were recorded using a CTD (CTD = conductivity, temperature, depth; Seabird Inc. SBE19).

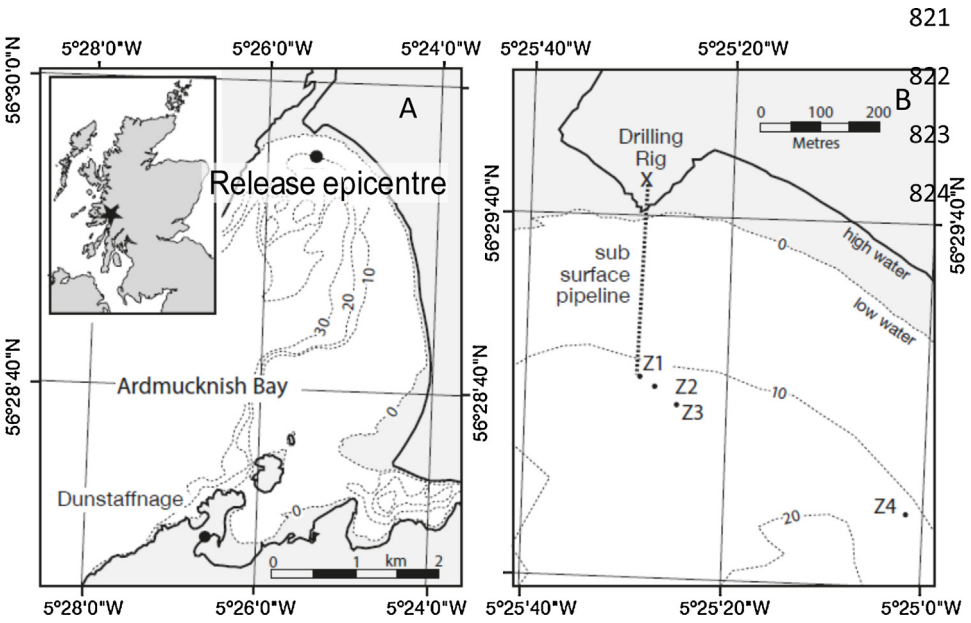

Fig. 1. (A) Location of Ardmucknish Bay in the west of Scotland. Black dot marks the CO_2 injection point at 11 m sediment depth (release epicentre); dotted lines are depth contours in metres. (B) Location of the sampling zones Z1–Z4 (Z = Zone) in relation to the CO_2 injection point (Zone 1). Modified after Taylor et al., (2015-b).

2.3. Analysis of marine sediments

The major and minor element composition of the sediments was determined by X-ray fluorescence (XRF, Philips MagiX-pro Wavelength dispersive X-ray fluorescence spectrometer, fitted with a 4 kW Rh end-window X-ray tube) on fused glass beads for the major elements and on pellets pressed into bricks for the minor elements (Croudace and Williams-Thorpe, 1988). Total inorganic carbon (TIC) and total carbon (TC) concentrations were measured with a CO_2 coulometer (Model CM5012, UIC Inc.), equipped with an Acidification Module (Model CM5130, UIC Inc.), and organic carbon (C_{org}) was calculated by subtracting the acid soluble fraction from the bulk carbon. Porosity was determined by mass difference between the wet sediment and sediment dried in the oven at 60 °C for a minimum of 72 h, assuming a sediment density of 2.6 g cm^{-3}. Grain size was measured on the dried sediments using a Malvern Mastersize analyser after shaking the samples overnight in a 1% Calgon solution to disaggregate them.

2.4. Analysis of seawater samples

Oxygen concentrations were determined using the Winkler titration technique (Winkler, 1888). DIC was measured using an Apollo SciTech DIC analyzer (AS-C3), using a LI-COR CO_2/H_2O (LI-7000) infrared analyser to detect CO_2 released from the sample after acidifying with 10% H_3PO_4. Total alkalinity was determined

Table 1
Details of geochemical sampling conducted during the QICS experiment. Z = Zone, DIC = dissolved inorganic carbon, TA = total alkalinity, C_{org} = organic carbon, TIC = total inorganic carbon.

	Prior to release	Release phase (May 17th–June 22nd 2012)		Recovery phase			
Sediment							
Day relative to start of injection	D-7/D-6	D13/D14	D34/D35	D41/D42	D53/D54	D125/D126	D356/D357/D358
Sampling date	10th/11th May 2012	30th/31st May 2012	20th/21st June 2012	27th/28th June 2012	9th/10th July 2012	19th/20th Sept. 2012	8th–10th May 2013
Pore fluid							
DIC/$\delta^{13}C_{DIC}$	Z1/Z2/Z3/Z4	Z1/Z2/Z3/Z4	Z1/Z2/Z3/Z4	Z1/Z2/Z3/Z4	Z1/Z2/Z3/Z4	Z1/Z2/Z3/Z4	Z1
TA	Z1/Z2/Z3/Z4	Z1/Z2/Z3/Z4	Z1/Z2/Z3/Z4	Z1/Z2/Z3/Z4	Z1/Z2/Z3/Z4	Z1/Z2/Z3/Z4	Z1/Z2/Z3/Z4
Nutrients	Z1/Z2/Z3/Z4	Z1/Z2/Z3/Z4	Z1/Z2/Z3/Z4	Z1/Z2/Z3/Z4	Z1/Z2/Z3/Z4	Z1/Z2/Z3/Z4	Z1/Z2/Z3/Z4
Anions	Z1/Z2/Z3/Z4	Z1/Z2/Z3/Z4	Z1/Z2/Z3/Z4	Z1/Z2/Z3/Z4	Z1/Z2/Z3/Z4	Z1/Z2/Z3/Z4	Z1/Z2/Z3/Z4
Cations	Z1	Z1	Z1/Z4	Z1/Z4	Z1	Z4	–
Methane	Z1/Z2/Z3/Z4	Z1/Z2/Z3/Z4	Z1/Z2/Z3/Z4	Z1/Z2/Z3/Z4	Z1/Z2/Z3/Z4	Z1/Z2/Z3/Z4	–
Sulphide	Z1/Z2/Z3/Z4	Z1/Z2/Z3/Z4	Z1/Z2/Z3/Z4	Z1/Z2/Z3/Z4	Z1/Z2/Z3/Z4	Z1/Z2/Z3/Z4	Z1/Z2/Z3/Z4
Solid phase							
Porosity	Z1/Z2/Z3/Z4	Z1/Z2/Z3/Z4	Z1/Z2/Z3/Z4	Z1/Z2/Z3/Z4	Z1/Z2/Z3/Z4	Z1/Z2/Z3/Z4	–
Grain size	Z1/Z2/Z3/Z4	Z1/Z2/Z3/Z4	–	Z1/Z2/Z3/Z4	Z1/Z2/Z3/Z4	–	–
Major and minor cations	–	Z1	–	Z1	Z1	–	–
C_{org}/TIC	Z1/Z4	–	Z1/Z4	Z1/Z4	Z1/Z4	–	–
Water column							
Sampling date	10th May 2012	31st May 2012	18th June 2012	27th June 2012	11th July 2012	18th Sept. 2012	
TA/DIC	Z1/Z2/Z3/Z4	Z1/Z2/Z3/Z4	Z1/Z2/Z3/Z4	Z1/Z2/Z3/Z4	Z1/Z2/Z3/Z4	Z1/Z2/Z3/Z4	–
Oxygen	Z1/Z2/Z3/Z4	Z1/Z2/Z3/Z4	Z1/Z2/Z3/Z4	Z1/Z2/Z3/Z4	Z1/Z2/Z3/Z4	Z1/Z2/Z3/Z4	–
Nutrients	Z1/Z2/Z3/Z4	Z1/Z2/Z3/Z4	Z1/Z2/Z3/Z4	Z1/Z2/Z3/Z4	Z1/Z2/Z3/Z4	Z1/Z2/Z3/Z4	–
CTD	Z1/Z2/Z3/Z4	Z1/Z2/Z3/Z4	Z1/Z2/Z3/Z4	Z1/Z2/Z3/Z4	Z1/Z2/Z3/Z4	Z1/Z2/Z3/Z4	–

by Gran titration (Gran, 1952) with the same analyzer (Apollo SciTech). The precision of the DIC and TA analyses (<±0.4%) is reported as the standard deviation of repeated measurements of the same seawater sample, and the accuracy was assessed by analysis of Certified Reference Materials (A. G. Dickson, Scripps (Dickson et al., 2007)). Nutrient concentrations were measured with a QuAAtro nutrient analyser. The precision of these measurements is ±0.027 μmol L^{-1} for PO_4 and ±0.109 μmol L^{-1} for Si, and detection limits are 0.004 μmol L^{-1} for PO_4 and 0.082 μmol L^{-1} for Si.

2.5. Analysis of pore waters

Cations were measured by inductively coupled plasma optical emission spectrometry (ICP–OES; Perkin-Elmer Optima 4300 DV) and by inductively coupled plasma mass spectrometry (ICP-MS; Thermo Scientific X-Series 2) after diluting samples by a factor of 50 with 0.04 N TD HNO_3. Standards were prepared from single element standard solutions that covered the expected range of concentrations. The reproducibility of the ICP–OES analyses, determined by replicate analysis of the same sample, is better than ±3% for all elements. Measured concentrations of a certified reference material seawater standard (CRM-SW; High Purity Standards) were within ±5% of the certified values for all elements except the transition metals, which have very low concentrations in CRM-SW relative to the pore waters.

Anions were measured by ion exchange chromatography (Dionex ICS2500) with 9 mmol L^{-1} Na_2CO_3 as the eluent. Repeat analysis of IAPSO (certified by the International Association for the Physical Sciences of the Oceans) seawater as well as single anion standards indicates that the reproducibility of the Cl and sulphate analyses is better than ±1%; for Br it is better than ±2%. The carbon isotopic composition of the DIC ($\delta^{13}C_{DIC}$) was determined using a multiflow preparation system coupled to an Isoprime continuous flow mass spectrometer at Royal Holloway University of London. Measurements were made by injecting 0.5 mL of water into vials containing orthophosphoric acid that had been flushed with helium and equilibrating the acid and water for 4 h at 40 °C (Mattey et al., 2008). $\delta^{13}C$ values were normalised to the V-PDB scale via a calibrated sodium bicarbonate internal standard and the standard deviation of 2 replicate measurements was less than ±0.3‰. The carbon isotopic composition of the injected CO_2 ($\delta^{13}C_{CO_2}$) was measured using a modified trace gas mass spectrometry system (Isoprime Ltd) (Fisher et al., 2006). Total alkalinity was determined by titration against 0.0005 mol L^{-1} HCl using a mixture of methyl red and methylene blue as an indicator. Analyses were calibrated against the IAPSO seawater standard and the reproducibility of the analyses was better than ±1%. DIC in pore waters was determined as described for water samples in Section 2.4. The precision of the analysis is usually better than ±0.1%, although for a few samples it was slightly less (up to ±0.4%). Total dissolved sulphide concentrations ($H_2S + HS^- + S^{2-}$) were determined using the diamine complexation method (Cline, 1969). Concentrations of methane were determined by gas chromatography (Agilent 7890 with FID) with a reported accuracy and precision of better than ±1%. Nutrient concentrations were determined after thawing and diluting the samples 20 times as described in Section 2.4. The precision of these measurements is ±0.015 μmol L^{-1} for PO_4, ±0.054 μmol L^{-1} for Si and ±0.34 μmol L^{-1} for NH_4, and detection limits are 0.007 μmol L^{-1} for PO_4, 0.095 μmol L^{-1} for Si and 0.2 μmol L^{-1} for NH_4.

3. Results

3.1. Chemical composition of the overlying water column

Variations in the chemical composition of the seawater samples that were collected before, during, and after the CO_2 injection are natural and mainly due to seasonal changes (Suppl. Table 6). Seawater temperature ranges from 9 to 14 °C, and salinity varies between 27 and 34 (Suppl. Fig. 1). These changes in salinity are due to mixing of brackish water from nearby Loch Etive with a salinity of 20–31, with higher salinity water (>34) transported into Ardmucknish Bay by tidal currents (Taylor et al., 2015-b) via nearby Loch Linnhe.

Concentrations of dissolved oxygen, phosphate and silicon show little variation with depth (Fig. 2), and concentrations of these species at Zone 1, the zone closest to the injection point, are generally similar to those recorded at Zones 2, 3 and 4. Stratification caused by the injection of the less saline and buoyant water from Loch Etive (Taylor et al., 2015-b), is only visible in the distribution of the dissolved species in September 2012, with slightly higher concentrations of phosphate and silicon at the sea surface in some zones. During the course of the sampling, natural seasonal variations in concentrations of oxygen (227–292 μmol L^{-1}, Fig. 2A–D), phosphate (0–0.5 μmol L^{-1}, Fig. 2E–H) and silicon (1–15 μmol L^{-1}, Fig. 2I–L) are observed. Highest nutrient concentrations and lowest oxygen concentrations are recorded in July 2012 (D53/D54) and September 2012 (D125/D126), 1 to 3 months after the CO_2 injection had stopped. Although oxygen super-saturated waters were occasionally recorded by in situ measurements within 30 cm of the seafloor during spring/summer 2012 (Atamanchuk et al., 2015), oxygen super-saturation is not found in the samples taken with the Niskin bottle 1 m of the seafloor.

DIC and TA concentrations were measured in samples recovered from closest to the seabed (about 1 m above seafloor) and these data are given in Table 2 together with pH values calculated from the DIC and TA measurements using CO2SYS (Pierrot et al., 2006). DIC and TA concentrations during the CO_2 injection period (D13/D14 and D34/D35, grey shaded area in Table 2) are within the range of values recorded both pre- and post-injection and similar to normal seawater. Thus, we find no evidence for the presence of injected CO_2 in the water column, at least in these samples. Calculated pH values (8.1–8.2) also remained within the normal range

Table 2
Results of analyses of carbonate system parameters in seawater samples collected from closest to the seafloor (~1 m above the seafloor). pH is calculated from DIC (dissolved inorganic carbon) and TA (total alkalinity) using CO2SYS (Pierrot et al., 2006) and equilibrium constants from (Mehrbach et al., 1973) as re-assessed by (Dickson and Millero, 1987). The grey shaded area indicates samples collected during the CO_2 injection phase. nd = not determined.

Sampling campaign	Zone 1 DIC (mmol L^{-1})/TA (mmol L^{-1})/$pH_{calc.}$	Zone 2 DIC (mmol L^{-1})/TA (mmol L^{-1})/$pH_{calc.}$	Zone 3 DIC (mmol L^{-1})/TA (mmol L^{-1})/$pH_{calc.}$	Zone 4 DIC (mmol L^{-1})/TA (mmol L^{-1})/$pH_{calc.}$
D-7/D-6	2.128/nd/nd	2.038/nd/nd	2.167/2.334/8.1	2.082/nd/nd
D13/D14	2.127/2.321/8.2	2.088/2.277/8.2	2.080/2.210/8.1	2.075/2.254/8.2
D34/D35	2.069/2.258/8.2	2.134/2.315/8.1	2.145/2.339/8.2	2.155/2.373/8.2
D41/D42	2.154/2.370/8.2	2.161/2.368/8.2	2.151/2.371/8.2	2.144/2.343/8.2
D53/D54	2.145/2.368/8.2	2.143/2.366/8.2	2.140/2.375/8.2	2.153/2.371/8.2
D125/D126	2.094/2.307/8.2	2.103/2.309/8.2	1.951/2.131/8.2	1.810/1.971/8.2

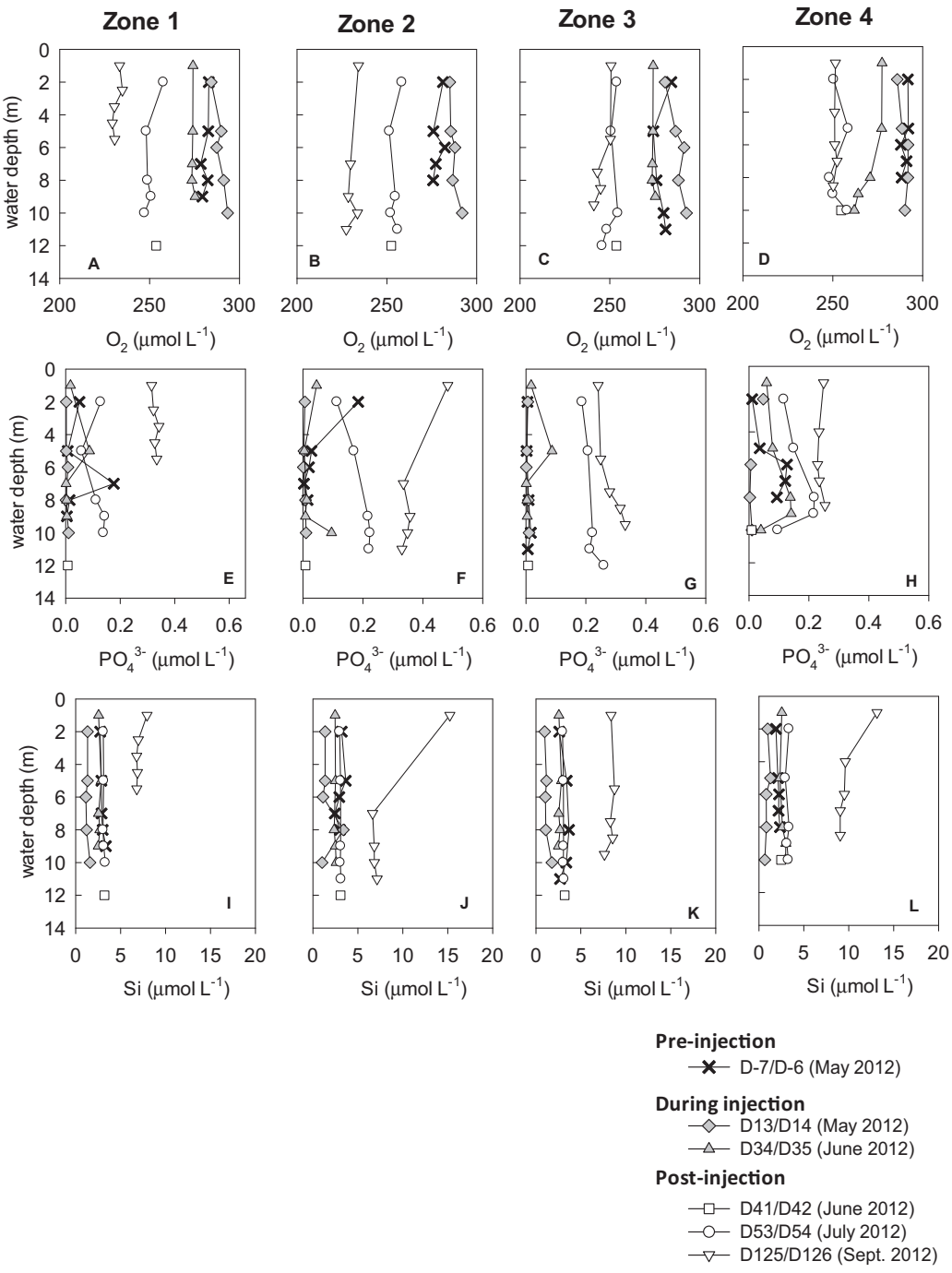

Fig. 2. Profiles of dissolved oxygen (A–D), phosphate (E–H) and dissolved silicon (I–L) measured in the water column over the course of the QICS experiment.

for seawater. The range of natural variability in Ardmucknish Bay is visible from the variations in DIC and TA concentrations in the months post-injection, which is comparable to variations recorded by in situ measurements of pCO_2 (300–400 µatm) (Atamanchuk et al., 2015).

3.2. Chemical composition and physical properties of the sediments

The grain size distribution of the Ardmucknish Bay sediments ranges from very fine to fine sands, and porosity is 50–60% in the uppermost 2 cm and 40–45% below (Table 5, Suppl. Table 3) and did not change during the course of the experiment. The total organic carbon content (C_{org}) of the sediments is low, ranging from 0.3 to 0.4% dry weight, and the total inorganic carbon content (TIC) of the sediments is also low (<0.1% dry weight) and close to the detection limit (Table 5, Suppl. Table4). The sediments are mainly composed of SiO_2 and Al_2O_3, with some K_2O, Na_2O, Fe_2O_3, CaO and MgO (1–3.1%), and minor amounts of TiO_2, MnO and P_2O_5 (<0.5%) (Fig. 3). There is little variation in the chemical composition of the sediments with depth, or before, during and after the CO_2 exposure (Suppl. Table 5). Concentrations of minor elements are generally low, with ~5 ppm Co, <20 ppm Pb, ~40 ppm Zn and ~45 ppm V. Cu is close to detection limit (2 ppm) and As and Ni are below the detection limit (2 ppm). Concentrations of minor elements are also similar before, during and after the release (Table 6).

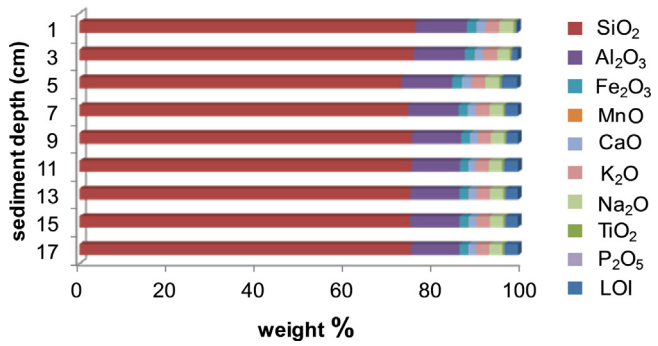

Fig. 3. Major element composition of sediments from Zone 1 on D13/D14. The composition of sediments collected from this location on D41/D42 and D53/D54 are very similar (Suppl. Table 5). LOI—loss on ignition.

3.3. Pore water geochemistry

Concentrations of all pore water species measured in Zone 1 to Zone 4 during the different sampling campaigns are given in Suppl. Tables 1 and 2.

3.3.1. Carbonate system parameters

Profiles of DIC, $\delta^{13}C_{DIC}$ and TA in sediment pore waters are shown in Fig. 4. Over the course of the experiment, there is little variation in DIC in pore waters from Zones 2–4 (i.e. >25 m away from the CO_2 injection point) with average (±standard deviation) values of 2.4 (±0.1) mmol L^{-1} (Table 3, Suppl. Table 1). However, in Zone 1, the area closest to the CO_2 injection point, substantial increases in DIC due to dissolution of the injected CO_2 are recorded in pore waters recovered on D34/D35 and D41/D42, i.e. 34/35 days after the CO_2 injection started and 5/6 days after the injection was stopped (Fig. 4A and B). Highest recorded DIC concentrations are more than 10 times higher than the background concentration (28.8 mmol L^{-1} compared to a background of 2.4 mmol L^{-1}); these are found in pore waters from below 14 cm sediment depth on D41/D42 (Fig. 4, Table 3). Above 14 cm, DIC concentrations of up to 8 mmol L^{-1} are measured (see also Blackford et al. 2014). Note that these are minimum values, because gaseous CO_2 can be lost during core retrieval if DIC concentrations are high. Between 2 and 3 weeks post-injection (D53/D54), the DIC concentrations in Zone 1 returned to close to pre-injection background values (Fig. 4B, Table 3). $\delta^{13}C_{DIC}$ values show a slight shift from around −2‰ to more negative values (−6‰) in Zones 2, 3 and 4 during the summer months (Fig. 4H–J). However, pore waters with high DIC concentrations (D34/D35 and D41/D42) from Zone 1 have much lower $\delta^{13}C_{DIC}$ values, as low as −20‰ (Fig. 4F). The carbon isotopic composition of the injected CO_2 is −26.6‰. The pore waters of Zone 1 with high DIC and low $\delta^{13}C_{DIC}$ values also have extremely high TA (up to 26.1 mmol L^{-1}, compared to a background of 2.5 (±0.3) mmol L^{-1} measured in Zones 2–4) (Fig. 4K–O, Table 3).

3.3.2. Cations and anions

In Zone 1 concentrations of some cations are also higher than average in pore waters with high DIC and TA, and low $\delta^{13}C_{DIC}$, i.e. pore waters sampled on D34/D35 and D41/D42 (Fig. 5, Table 3). These samples have high Ca concentrations (up to 18.6 mmol L^{-1} compared to average values of 9.9 mmol L^{-1}) (Fig. 5A and B, Table 3), and concentrations of B, Sr and Li are up to 1.2, 1.4 and 3 times higher than average background, respectively (Fig. 5C–F, Table 3). In addition, concentrations of Mn and Fe are up to an order of magnitude higher in the high DIC pore waters of Zone 1 (Fig. 5G–J, Table 3). Concentrations of Al and Ba are also slightly higher than average in the high DIC pore waters (Table 3), but no significant increase in concentrations of K, Na or Rb was observed in pore waters with high DIC (Table 4). Concentrations of Y, V, Cu, Zr, Cd, Ag, Hg, Pb, Sn and Ti were always close to or below detection limit. In Zone 1 concentrations of all cations returned to close to background values by D53/D54, i.e. 2–3 weeks after the injection of CO_2 was stopped (Fig. 5, Table 3). By contrast, concentrations of most cations measured in pore waters from Zone 4, furthest away from the CO_2 injection point, were close to seawater values before, during and after the CO_2 injection (Fig. 5, Table 3, Supplementary Table 2). Concentrations of dissolved iron (up to 7 µmol L^{-1}, Fig. 5H) and dissolved manganese (up to 7 µmol L^{-1}, Fig. 5J) are nevertheless slightly higher in pore waters in the uppermost 5 cm of the sediments, due to remineralisation of organic material (Canfield et al., 1993).

Concentrations of the anions Cl, Br, and sulphate showed only slight variations over the course of the sampling campaign, and concentrations are similar in all 4 sampling zones. There are

Table 3
Chemical composition of pore waters collected from Zone 4 (reference) compared to pore waters collected from Zone 1 (sediments less than 25 m away from the CO_2 injection point). Data for Zone 4 are the average (±standard deviation) and maximum value of all data obtained for campaigns D34/D35, D53/D54 and D125/D126. Data for Zone 1 are the average (±standard deviation) and maximum value for all data obtained for that core. The grey shaded area indicates sampling campaigns with elevated pore water DIC concentrations. Numbers given in bold depict species that have higher concentrations in the high DIC pore waters. Seawater values are from Turekian (1968) (*) or from the OSPAR convention for the protection of the marine environment (2006) (**). The former values are for ocean standard seawater; the latter values are for the Northern North Sea. nd = not determined

	Zone 4 average maximum	**Zone 1** D-7/D-6 average maximum	**Zone 1** D34/D35 average maximum	**Zone 1** D41/D42 average maximum	**Zone 1** D53/D54 average maximum	**Seawater**
DIC (mmol L^{-1})	2.3 (±0.2) 2.3	2.3 (±0.1) 2.4	**4.0** (±2.4) 10.3	**11.4** (±10.4) 28.8	2.6 (±0.1) 3.1	-
TA (mmol L^{-1})	2.3 (±0.1) 2.7	2.4 (±0.1) 2.4	**3.7** (±2.3) 10.1	**10.7** (±7.6) 26.1	2.8 (±0.3) 3.4	-
Mg (mmol L^{-1})	50.2 (±1.2) 52.3	51.0 (±0.8) 51.7	**51.9** (±0.2) 52.3	**51.7** (±0.7) 52.8	50.7 (±0.5) 51.6	54*
Ca (mmol L^{-1})	9.4 (±0.4) 10.0	9.7 (±0.2) 9.9	**10.4** (±0.7) 12.4	**13.3** (±3.3) 18.6	9.9 (±0.2) 10.1	10.4*
Ammonium (µmol L^{-1})	89 (±31) 150	56 (±2) 64	59 (±11) 95	**178** (±68) 333	104 (±27) 144	-
B (µmol L^{-1})	419 (±11) 434	461 (±16) 471	454 (±11) 480	**471** (±54) 567	442 (±14) 461	417*
Si (µmol L^{-1})	68 (±8) 86	61 (±7) 70	77 (±8) 87	55 (±25) 154	78 (±7) 93	105*
Sr (µmol L^{-1})	89 (±2) 94	91 (±1) 92	**95** (±2.3) 101	**104** (±11) 122	91 (±2) 94	94*
Li (µmol L^{-1})	27 (±5) 34	29 (±5) 35	**42** (±5) 54	**53** (±21) 82	35 (±6) 49	25*
Mn (µmol L^{-1})	4 (±3) 13	7 (±1) 17	**11** (±9) 36	**19** (±13) 49	10 (±2) 6	0.0011–0.0028**
Fe (µmol L^{-1})	4 (±7) 7	4 (±2) 7	**10** (±6) 47	**36** (±49) 162	7 (±6) 18	0.004–0.11**
Al (µmol L^{-1})	0.8 (±0.6) 2.2	1.1 (±0.3) 1.5	0.8 (±0.4) 1.4	**1.3** (±0.7) 2.5	1 (±0.8) 2.3	0.01*
Ba (µmol L^{-1})	0.15 (±0.03) 0.21	0.12 (±0.02) 0.15	**0.16** (±0.2) 0.19	**0.20** (±0.2) 0.26	0.13 (±0.3) 0.18	0.15*
Mo (µmol L^{-1})	0.2 (±0.1) 0.6	0.2 (±0.1) 0.3	0.2 (±0.1) 0.3	0.2 (±0.3) 0.9	0.3 (±0.1) 0.5	0.001*
Cr (nmol L^{-1})	9 (±11) 31	47 (±41) 120	26 (±11) 44	20 (±15) 56	nd	2** (Atlantic Ocean)
Sb (nmol L^{-1})	19 (±16) 61	12 (±13) 41	13 (±13) 35	8 (±7) 20	nd	3*

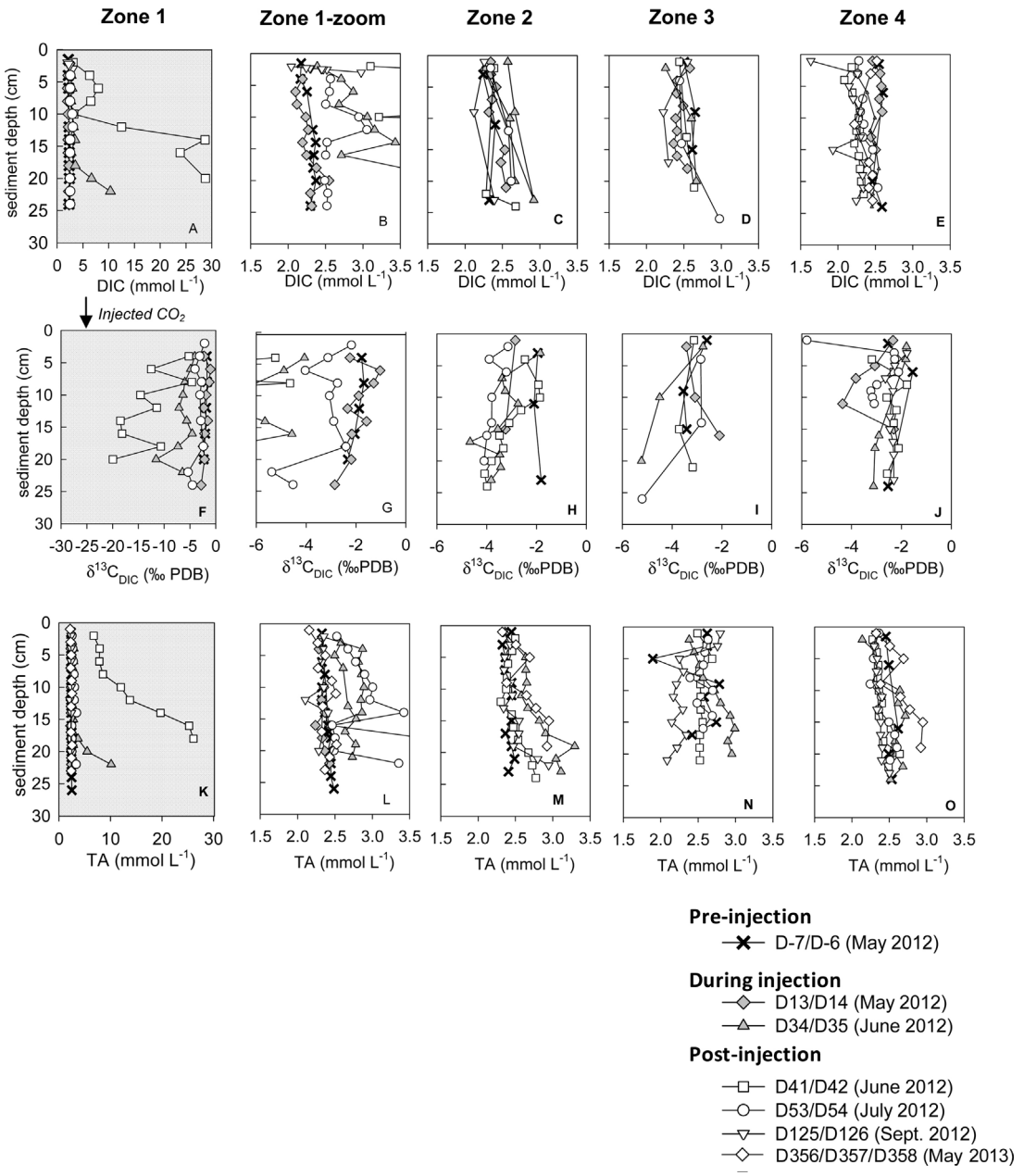

Fig. 4. Profiles of pore water DIC, $\delta^{13}C_{DIC}$ and TA over the course of the QICS experiment. Note that the scales on the horizontal axis for Zone 1 (panels A, F and K) are different from the scales used on the rest of the panels. The arrow in panel F indicates the isotopic compositions of the injected CO_2 gas.

Table 4
Pore water concentrations for chemical species that show little variation over the course of the QICS experiment in all four zones. Data are given as the average concentration (±standard deviation) measured in each zone during all sampling campaigns. bd = below detection limit, nd = not determined. Seawater values are from Turekian (1968).

Species	**Zone 1** average (mmol L^{-1})	**Zone 2** average (mmol L^{-1})	**Zone 3** average (mmol L^{-1})	**Zone 4** average (mmol L^{-1})	**Seawater** (mmol L^{-1})
Cl	543 (±51)	531 (±74)	541 (±81)	521 (±40)	553
Sulphate	28 (±2)	27 (±4)	28 (±4)	27 (±2)	28
Br	0.83 (±0.07)	0.81 (±0.11)	0.83 (±0.12)	0.77 (±0.06)	0.849
Rb	1.3 e^{-3} (±0.5 e^{-4})	nd	nd	1.3 e^{-3} (±1.1 e^{-4})	1.4 e^{-3}
K	10 (±0.2)	nd	nd	10 (±0.3)	10
Na	411 (±6)	nd	nd	406 (±8)	474
Sulphide	bd	bd	bd	bd	–
Methane	<1 e^{-3}	<1 e^{-3}	<1 e^{-3}	<1 e^{-3}	–

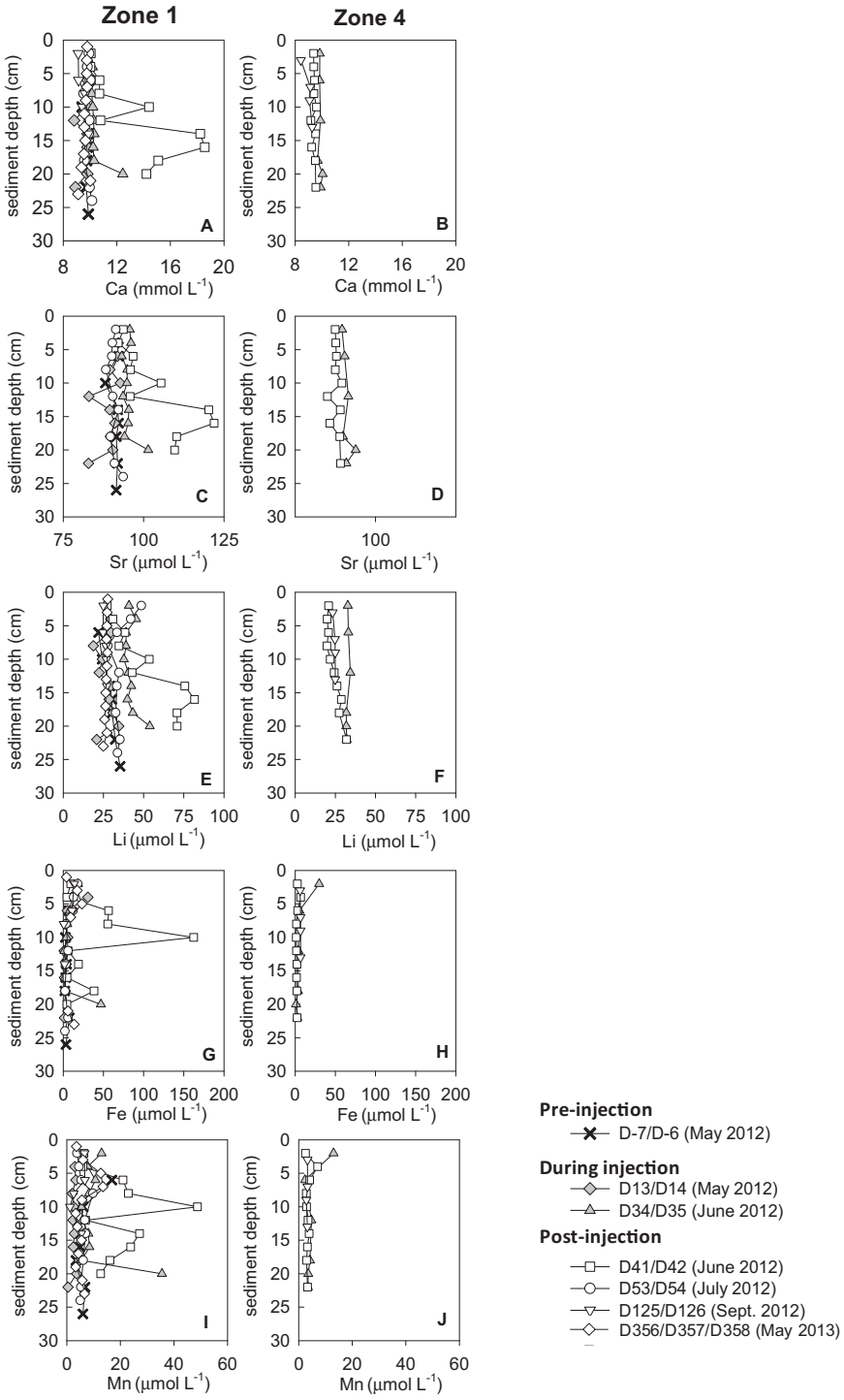

Fig. 5. Profiles of pore water cations Ca, Sr, Li, Fe and Mn over the course of the QICS experiment in Zone 1 (sediments less than 25 m away from the CO_2 injection point) compared to Zone 4.

no significant changes in the concentrations of these variables with depth in the sediment column, and average values for the upper 20–25 cm of the sediments are given in Table 4. Sulphide concentrations are always below detection limit and methane concentrations are low (<1 µmol L^{-1}).

3.3.3. Nutrients

In all 4 sampling zones, concentrations of dissolved silicon varied between ~50 and ~100 µmol L^{-1}, phosphate concentrations varied between ~3 and ~10 µmol L^{-1} and ammonium varied between ~100 and ~150 µmol L^{-1} (Fig. 6). There is some natural variation in nutrient concentrations with site and with season, and lowest concentrations of pore water nutrients were found in May (in both 2012 and 2013). However, concentrations of dissolved silicon and ammonium appear to be higher than average in pore waters sampled from Zone 1 on D41/D42; these pore waters have high DIC concentrations due to dissolution of injected CO_2 (Fig. 6A and I).

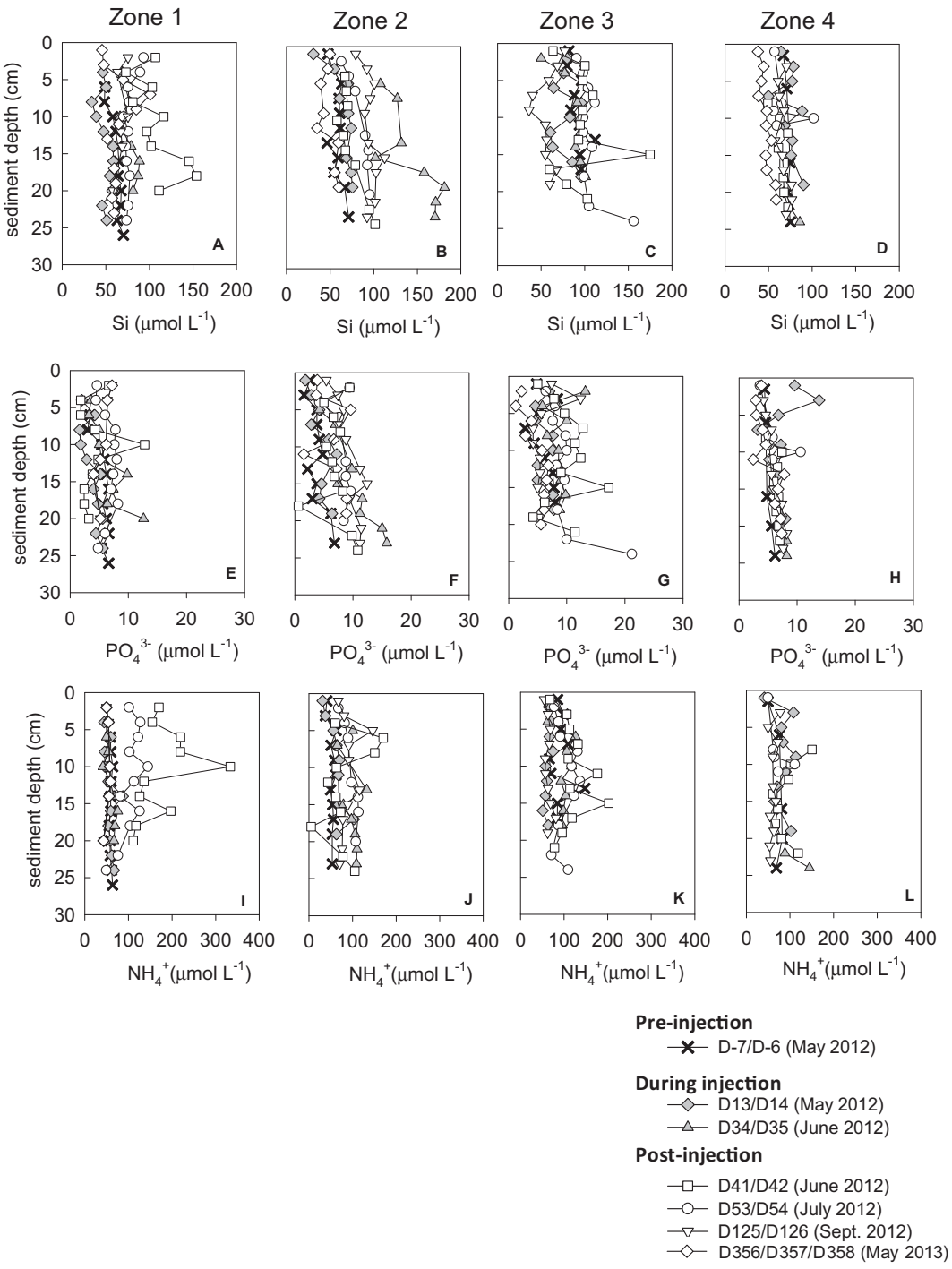

Fig. 6. Profiles of pore water nutrient concentrations during the course of the QICS experiment.

4. Discussion

Ardmucknish Bay is a normal-productivity marine environment with seabed sediments that consist of fine grained sands that have low organic carbon content. The chemical composition of the sediments is typical for sandy marine environments (Tables 5 and 6), and comparable to the composition of sediments in the North Sea (Table 6), where the greatest opportunity for offshore CCS lies within Europe. The chemical composition of pore waters in the near-surface sediments of the bay prior to the injection of CO_2 is similar to that of the overlying seawater, with the exception of some metals (e.g. Fe, Mn) and nutrients, which typically have higher levels in the pore waters than they do in the water column. Concentrations of pore water nutrients show some variation over the summer months (Fig. 6), which is typical for near-surface coastal sediments and is the result of seasonal changes and natural heterogeneity in the supply of organic carbon from the water column (Klump and Martens, 1989). Increased carbon remineralisation during the summer is demonstrated by slightly increased concentrations of dissolved iron (up to 7 µmol L^{-1}, Fig. 5H) and dissolved manganese (up to 7 µmol L^{-1}, Fig. 5J) in pore waters in the uppermost 5 cm of the sediment. Remineralisation of organic carbon is also indicated by pH profiles measured in the upper centimetre of the sediment (Taylor et al., this issue-a). Nevertheless,

Table 5
Properties of sediments from Ardmucknish Bay. Data are given as the average (±standard deviation) of all measurements made in each zone over the course of the experiment. For details see Suppl. Tables 3 and 4. Grain size of 63–125 μm: very fine sand, 125–250 μm: fine sand. TIC = total inorganic carbon, C_{org} = organic carbon, cmbsf = centimetres below seafloor, nd = not determined.

	Zone 1 average	**Zone 2** average	**Zone 3** average	**Zone 4** average
Porosity				
0–2 cmbsf	0.49 (±0.03)	0.51 (±0.03)	0.56 (±0.06)	0.53 (±0.03)
16–18 cmbsf	0.43 (±0.01)	0.44 (±0.01)	0.46 (±0.01)	0.44 (±0.01)
Grain size (μm)				
0–2 cmbsf	137 (±10)	127 (±11)	118 (±11)	142 (±10)
16–18 cmbsf	135 (±2)	126 (±2)	117 (±3)	140 (±3)
TIC (% dry weight)				
0–2 cmbsf	0.08 (±0.01)	nd	nd	0.04 (±0.01)
16–18 cmbsf	0.09 (±0.01)	nd	nd	0.03 (±0.03)
C_{org} (% dry weight)				
0–2 cmbsf	0.3 (>±0.1)	nd	nd	0.4 (>±0.1)
16–18 cmbsf	0.3 (>±0.1)	nd	nd	0.4 (>±0.1)

rates of organic carbon remineralisation are insufficient to cause measureable increases in pore water DIC concentrations in the near-surface sediments (Fig. 4C–E, Table 3). The changes in concentrations of nutrients and some cations, together with minor changes in Cl and sulphate concentrations (Table 4, Supplementary Table 1) are principally the result of natural changes in salinity (Taylor et al., 2015-b), and/or seasonal variations in the rate of supply and remineralisation of organic carbon, and are not related to CO_2 leakage.

The QICS experiment demonstrates that injection of CO_2 into marine sediments can induce localised, transient changes in the geochemistry of the near surface pore waters. Although release of CO_2 gas into the water column in the form of bubble streams was observed within hours of the start of the CO_2 injection (Blackford et al., 2014), changes in pore water chemistry were not recorded until 5 weeks after the start of the CO_2 injection (Fig. 4), and largest changes were observed about 1 week after the injection was stopped (Figs. 4–6). This reflects the much slower movement of the dissolved CO_2 through the pore waters, relative to CO_2 in the gas phase. Where the CO_2 enriched pore fluids reach the surface sediments, total alkalinity increases by up to an order of magnitude (Fig. 4), there is release of cations including Ca, Sr, Li, Fe and Mn (Fig. 5), and concentrations of the nutrient elements including dissolved silicon and ammonium are also increased (Fig. 6). However, these changes are spatially restricted, and are only recorded in pore waters from Zone 1; that is, less than 25 m away from the CO_2 injection point. Concentrations of all pore water constituents nevertheless returned to background values 2–3 weeks after the injection was stopped, indicating that the impact of the injected CO_2 was short-lived. During later sampling campaigns, there was no evidence for lateral spread of the dissolved CO_2 into near surface pore waters into adjacent Zones (Zones 2–4), i.e. into sediments located >25 m away from the injection point.

Evidence that the increase in the DIC concentration observed in the pore waters recovered from Zone 1 was caused by the injected CO_2, comes from the carbon isotopic composition of the DIC ($\delta^{13}C_{DIC}$, Fig. 4). Pore waters with high DIC concentrations are enriched in ^{12}C, with $\delta^{13}C_{DIC}$ values of −20‰ compared to −2‰ for pore waters from this zone pre-injection. The injected CO_2 has a $\delta^{13}C$ value of −26.6‰, indicating that the DIC-rich pore waters consist of a mixture of biogenic 'background' DIC and DIC derived from dissolution of the injected CO_2 (see also Blackford et al., 2014). Much smaller shifts in $\delta^{13}C_{DIC}$ values, to about −4 to −6‰, are occasionally recorded in all 4 sampling zones. These are likely due to in situ production of $^{12}CO_2$ during the remineralisation of organic matter, which is generally depleted in ^{13}C with $\delta^{13}C$ values ranging from −32 to −10‰ for plants and marine plankton (Zeebe and Gladrow, 2001).

A key concern is that leakage of CO_2-rich fluids from CCS reservoirs could result in the release of toxic metals from the overlying marine sediments. Processes controlling metal release into pore waters at elevated CO_2 concentrations include mineral dissolution and desorption of cations from mineral surfaces (Ardelan and Steinnes, 2010; Kirsch et al., 2014; Wunsch et al., 2014, 2013). During the QICS experiment, concentrations of a number of metals, including Ca, Fe and Mn, and the metalloid Si, increased in the

Table 6
Concentrations of metals in sediments collected from Zone 1 on D13/D14, D42/D43 and D53/D54. Data are given as the average (±standard deviation) of all samples collected from the upper 18 cm of each core. Data for North Sea sediments are from Stevenson (2001), sediment quality guideline values are from Long et al. (1995), and metal concentrations in North Sea drill cuttings are from Breuer et al. (2004). LOD = limit of detection, bd = below detection limit, nd = not determined.

	As (ppm)	Ba (ppm)	Co (ppm)	Cr (ppm)	Cu (ppm)	Ni (ppm)	Pb (ppm)	V (ppm)	Zn (ppm)
Zone 1 D13/D14	bd (LOD = 2)	668 (13)	5 (±0)	11 (±3)	2 (±1)	bd (LOD = 2)	16 (±1)	45 (±3)	39 (± 3)
Zone 1 D42/D43	bd (LOD = 2)	674 (15)	5 (±0)	14 (±7)	3 (±1)	bd (LOD = 2)	16 (±1)	46 (±3)	37 (± 2)
Zone 1 D53/D54	bd (LOD = 2)	660 (19)	5 (±0)	12 (±4)	1 (±1)	bd (LOD = 2)	15 (±1)	44 (±2)	41 (± 2)
North Sea *muddy sediments*	nd	442	9	73	13	32	23	34	82
North Sea *sandy sediments*	nd	335	5	34	3	13	14	19	25
Guideline values									
Rarely associated with effects	<8.2	nd	nd	<81	<34	<20.9	<46.7	nd	<150
Occasionally associated with effects	8.2–70	nd	nd	81–370	34–270	20.9–51.6	46.7–218	nd	150–410
Frequently associated with effect	>70	nd	nd	>370	>270	>51.6	>218	nd	>410
North Sea drill cuttings	nd	22600	nd	426	374	137	4790	523	2510

high-DIC pore waters (Fig. 5, Table 3). At the same time, TA increased. This is consistent with weathering of mineral phases by the dissolved CO_2, including carbonates, silicates and Fe and Mn-oxides and -sulphides, which have been shown to release cations during short-term exposure to high-CO_2 conditions (Ardelan and Steinnes, 2010; Kirsch et al., 2014; Mickler et al., 2013). Concentrations returned to close to background values by D53/D54, i.e. 2–3 weeks after the injection of CO_2 was stopped, probably due to a combination of flushing of the permeable sandy sediments with overlying seawater, re-precipitation of minerals in the uppermost sediments and sinking of the denser CO_2-rich pore water (Blackford et al., 2014).

Considered together, high Ca concentrations, high TA and high concentrations of metals typically incorporated in carbonates (Li, Sr, Ba, B), indicate that dissolution of sedimentary carbonate is principally responsible for the changes in pore water geochemistry. Nevertheless, there is no clear change in total inorganic carbon (TIC) content of the sediments (Table 5). This is consistent with the results of laboratory experiments, which show that dissolution of carbonates is the primary source of released metals even in sandstone aquifers that have very low carbonate concentrations (Kirsch et al., 2014). The absolute increase in the concentration of dissolved silicon is much smaller than the absolute increase in levels of pore water Ca (Table 3), implying that the silicate dissolution rate is much lower than the carbonate dissolution rate. This is also in agreement with laboratory experiments which demonstrate that silicate dissolution rates can be ~2 orders of magnitude slower than carbonate dissolution (Mickler et al., 2013).

In the localised area where the injected CO_2 reached the near surface sediments (Zone 1), absolute concentrations of metals in pore waters that are perceived to be the most environmentally and toxicologically significant, such as Cu, Ag, Cd, Hg, Sn, Pb, and Cr, were mostly close to detection limit or low compared to heavily polluted environments (Bryan and Langston, 1992). Some of these metals may be present as impurities in carbonates and are released into solution when carbonate dissolves (Kirsch et al., 2014; Wunsch et al., 2013); additionally, some of these metals co-precipitate with Fe–Mn oxyhydroxides and sulphides, or are present in silicate minerals, all of which can be dissolved in the presence of high CO_2 (Mickler et al., 2013).

The extent of metal leaching depends not only on CO_2 concentrations and pH, but it is also a function of the amount of heavy metals present in the sediment. Concentrations of environmentally harmful metals in Ardmucknish Bay sediments are generally low and always lower than the threshold for quantitative environmental quality guidelines often used for marine sediments and estuaries defined by Long et al. (1995) (Table 6). Similarly, most proposed sub-seabed CCS sites, at least in the North Sea, are overlain by surface sediments that mainly consist of sands and mud and have low levels of trace metals (Stevenson, 2001), Table 6. Nevertheless, the overall increase in pore water metal concentrations in the QICS experiment, even at low CO_2 leakage rates (Table 5), indicates that release of metals will occur and concentrations can be expected to be significantly higher at higher leakage rates and/or leakage duration. Moreover, if sites are contaminated by, for example, drill cuttings that can have order of magnitude higher metal contents than normal sediments (Breuer et al., 2004) (Table 6), or they are located in polluted areas such as the proposed CO_2 storage site in Suances (N-Spain) estuary, then the potential for release of harmful levels of metals may be higher still (Payán et al., 2012; Basallote et al., 2014).

Microbiological studies indicate that the abundances of microbes and cyanobateria decreased (Tait, 2015) and the diversity and abundance of macrofauna declined (Widdicombe et al., 2015) as a result of CO_2 reaching the near-surface sediments in Zone 1. As our data indicate that there were only minor changes in heavy metal concentrations in the pore waters with high DIC, it seems likely that these changes in the microbial and faunal community structures are most probably linked to elevated CO_2 rather than elevated metal concentrations. Advection of anoxic, sulphidic and, in the case of a leakage from a saline aquifer, highly saline pore waters displaced by CO_2 may pose an additional threat to benthic ecosystems (Caroll et al., 2014). However, during the QICS experiment, sulphide concentrations always remained below detection limit, and low methane and constant chloride concentrations suggest that the surface sediments in Ardmucknish Bay were not affected by advection of fluids from other sources. Previously, in situ benthic chamber experiments conducted at 5000 μatm CO_2 (Ishida et al., 2013) indicate that rates of sulphate reduction and methanogenesis are enhanced in the presence of elevated CO_2. We find no evidence for this in the Ardmucknish Bay pore waters and concentrations of sulphate are close to values of overlying water. This is probably because the organic carbon content of the sediments is low (<0.6%), so sulphate reduction and methanogenesis only occur at depth or not at all.

Streams of CO_2 bubbles were observed venting from the sediments into the water column within hours of the start of the CO_2 injection, and ~15% of the injected CO_2 was estimated to be released as CO_2 gas directly into the water column. pCO_2 concentrations of up to 1250 μatm were recorded just above the seafloor in the close vicinity of the bubble streams, compared to background values of about 360–370 μatm (Atamanchuk et al., 2015). Nevertheless, the absence of any increase in DIC or TA in seawater samples collected using the Niskin bottles from ~1 m above the seafloor (Table 2) indicates that the impact of bubble dissolution is highly localised in space and time. This is confirmed by pCO_2 sensor measurements from 1 m above the seafloor that showed only very localised increase of pCO_2 in Zone 1 (Atamanchuk et al., 2015). Although there is no geophysical evidence for the lateral spread of CO_2 in the subsurface sediments away from Zone 1 (Cevatoglu et al., 2015), alterations in microbial abundances were observed in sediments from Zone 2, which is located more than 25 m away from the injection point (Tait, 2015). This raises the possibility that CO_2-enriched bottom waters could infiltrate the surface sediments beyond Zone 1. We find no evidence for increased TA or DIC in the pore waters in sediments from Zone 2 throughout the duration of the QICS experiment. This may mean that the microbes either react very quickly to small and transient changes in CO_2 in the water column, or that they react to parameters other than the chemical composition of the sediment pore waters. In any case, our data demonstrate that the chemical composition of the pore waters even in Zone 1 rapidly returns to background levels within 2 weeks of the end of the CO_2 injection, as does the biology (Tait, 2015; Widdicombe et al., 2015).

Most proposed and operational offshore CCS sites are in shelf sea environments with water depths of between 30 and 300 m (e.g. Sleipner (110 m)). At these water depths, with minimum bottom water temperatures of around 3–4 °C, any CO_2 that leaks from the storage reservoir and reaches the surface sediments will either be in the gas phase, or dissolved in the sediment pore waters, as it was in our experiment (Blackford et al., 2015). Our study demonstrates that once leakage is detected, collection of sediment cores and chemical analysis of pore water constituents is essential for establishing the impact of leakage on the marine ecosystem due to changes in carbonate system, nutrient and metal dynamics in the near-surface, and for assessing the effects of carbonate buffering. Additionally, our $\delta^{13}C_{DIC}$ analyses also demonstrate that if the stable carbon isotopic composition of the leaked CO_2 is significantly different from background seawater, then this may be a useful tracer of the CO_2 source. However, it is clear that localised and transient changes in water column CO_2 concentra-

tions cannot be adequately detected by ship-based sampling. To this end, in situ measurements, for example using pCO_2 sensors (Atamanchuk et al., 2015), are much more useful. Our study also highlights the importance of establishing a chemical baseline for the near-surface sediments and their pore waters, and the water column, which takes into account the natural spatial and temporal heterogeneity in shelf seas driven by biological and physical processes such as carbon supply and remineralisation, variations in freshwater input and mixing. Detailed recommendations for geochemical monitoring at a CCS site, based on results from the QICS experiment, can be found in Blackford et al. (2015).

5. Conclusions

In order to assess the potential effects of leakage of CO_2 from subseafloor CCS reservoirs on the geochemistry of benthic ecosystems, and to determine the footprint of any changes, the chemical composition of shallow marine sediments, their pore waters and the overlying water column has been determined before, during and after a field-scale CO_2 release experiment. The total amount of CO_2 injected into the sediments was relatively small (4.2 t over 37 days), but is comparable to leakage from for example an abandoned well (200 t yr^{-1}, IEA, 2008) or through small fractures (<170 to 3800 t yr^{-1}; Klusman, 2003). Nevertheless, pronounced changes in the chemical composition of the pore waters in sediment are observed. The injected CO_2 has a low $\delta^{13}C$ composition (−26.6‰), and dissolution of this CO_2 into the pore waters results in low $\delta^{13}C_{DIC}$ values (as low as −20‰, compared to background values of ∼−2‰) and increased concentrations of DIC and TA. Concentrations of Ca, Li, Sr, Ba, Si and B are also higher than background, indicating dissolution of sediment phases. Although carbonates are the main source of metals released to the pore waters affected by the injected CO_2, the carbonate content of the sediments in Ardmucknish Bay is relatively low, so higher metal concentrations may be expected as a result of leakage from CCS reservoirs in other marine settings that have higher carbonate concentrations in the overlying sediments.

The extent of metal release that we observe is not sufficient to be considered as harmful for the benthic environment, as concentrations of released metals were very low, transient and spatially restricted. Nevertheless, it is clear from the QICS experiment that leakage of CO_2 results in rapid mobilisation of metals, and that increased levels of dissolved CO_2 lead to changes in microbial diversity and the composition of the benthic fauna. Thus, leakage of CO_2 through sediments that have higher metal concentrations, and higher/longer leakage, may well be detrimental to the environment.

During the release experiment, the footprint of the geochemical changes to the sediment pore waters was restricted to an area close to the CO_2 injection point. Nevertheless, our data clearly demonstrate that the impact of CO_2 on the benthic ecosystem is not confined to seafloor features, such as pockmarks and gas bubbles streams that are easily recognised using conventional monitoring tools. The changes in the chemical composition of the pore waters, however, are likely to be short-lived, returning to background levels within weeks once the CO_2 release is stopped.

Acknowledgments

This work was funded by UK Natural Environment Research Council (NERC) grant NE/H013962/1 and the Scottish Government. We thank Belinda Alker, Peter Taylor, Darryl Green, Carolyn Graves, James Hunt, Sarah Wright and Ambra Milani for field and technical support, and Kate Davis for help with drafting the figures. We also thank the NERC National Facility for Scientific Diving located at the Scottish Association for Marine Science (SAMS) for collecting the cores and the crew of the R. V. *Seòl Mara* and John Montgomery at SAMS for providing operational support. Special thanks are due to the land-owners (Lochnell Estate) and users (Tralee Bay Holiday Park) for allowing us to conduct the experiment on their premises. We gratefully acknowledge constructive comments from two anonymous reviewers, which have helped to improve the manuscript.

Appendix A. Supplementary data

Supplementary data associated with this article can be found, in the online version, at doi:10.1016/j.ijggc.2014.10.[j.ijggc.2014.10.008]008

References

Ardelan, M.V., Steinnes, E., 2010. Changes in mobility and solubility of the redox sensitive metals Fe, Mn and Co at the seawater-sediment interface following CO_2 seepage. Biogeosciences 7, 569–583.

Atamanchuk, D., Tengberg, A., Aleynik, D., Fietzek, P., Hall, P.O.J., Shitashima, K., Lichtschlag, A., Stahl, H., 2015. Detection of CO_2 leakage from a simulated subseabed storage site using three different types of pCO2 sensors. Int. J. Greenhouse Gas Control 38, 121–134.

Bachu, S., Adams, J.J., 2003. Sequestration of CO_2 in geological media in response to climate change: capacity of deep saline aquifers to sequester CO_2 in solution. Energy Convers. Manage. 44, 3151–3175.

Bachu, S., Watson, T.L., 2009. Review of failures for wells used for CO_2 and acid gas injection in Alberta, Canada. Energy Procedia 1, 3531–3537.

Basallote, M.D., De Orte, M.R., DelValls, T.Á., Riba, I., 2014. Studying the effect of CO_2-induced acidification on sediment toxicity using acute amphipod toxicity test. Environ. Sci. Technol. 48, 8864–8872.

Bednarsek, N., Tarling, G.A., Bakker, D.C.E., Fielding, S., Jones, E.M., Venables, H.J., Ward, P., Kuzirian, A., Leze, B., Feely, R.A., Murphy, E.J., 2012. Extensive dissolution of live pteropods in the Southern Ocean. Nat. Geosci. 5, 881–885.

Blackford, J., Stahl, H., Bull, J.M., Bergès, B.J.P., Cevatoglu, M., Lichtschlag, A., Connelly, D., James, R.H., Kita, J., Long, D., Naylor, M., Shitashima, K., Smith, D., Taylor, P., Wright, I., Akhurst, M., Chen, B., Gernon, T.M., Hauton, C., Hayashi, M., Kaieda, H., Leighton, T.G., Sato, T., Sayer, M.D.J., Suzumura, M., Tait, K., Vardy, M.E., White, P.R., Widdicombe, S., 2014. Detection and impacts of leakage from sub-seafloor carbon dioxide storage. Nat. Clim. Change 4, 1011–1016, http://dx.doi.org/10.1038/nclimate2381, in press.

Blackford, J., Bull, J.M., Cevatoglu, M., Connelly, D., Hauton, C., James, R.H., Lichtschlag, A., Stahl, H., Widdicombe, S., Wright, I.C., 2015. Marine baseline and monitoring strategies for carbon dioxide capture and storage (CCS). Int. J. Greenhouse Gas Control 38, 221–229.

Blackford, J., Jones, N., Proctor, R., Holt, J., Widdicombe, S., Lowe, D., Rees, A., 2009. An initial assessment of the potential environmental impact of CO_2 escape from marine carbon capture and storage systems. Proc. Inst. Mech. Eng., A: J. Power Energy 223, 269–280.

Breuer, E., Stevenson, A.G., Howe, J.A., Carroll, J., Shimmield, G.B., 2004. Drill cutting accumulations in the Northern and Central North Sea: a review of environmental interactions and chemical fate. Mar. Pollut. Bull. 48, 12–25.

Bryan, G.W., Langston, W.J., 1992. Bioavailability, accumulation and effects of heavy metals in sediments with special reference to United Kingdom estuaries: a review. Environ. Pollut. 76, 89–131.

Burnside, N.M., Shipton, Z.K., Dockrill, B., Ellam, R.M., 2013. Man-made versus natural CO_2 leakage: A 400 k.y. history of an analogue for engineered geological storage of CO_2. Geology 41, 471–474.

Canfield, D.E., Thamdrup, B., Hansen, J.W., 1993. The anaerobic degradation of organic matter in Danish coastal sediments: iron reduction, manganese reduction, and sulfate reduction. Geochim. Cosmochim. Acta 57, 3867–3883.

Caroll, A.G., Przeslawski, R., Radke, L.C., Black, J.R., Picard, K., Moreau, J.W., Haese, R.R., Nichol, S., 2014. Environmental considerations for subseabed geological storage of CO_2: a review. Cont. Shelf Res. 83, 116–128.

Cevatoglu, M., Bull, J.M., Vardy, M.E., Gernon, T.M., Wright, I., Long, D., 2015. Gas migration pathways, controlling mechanisms and changes in sediment physical properties observed in a controlled sub-seabed CO_2 release experiment$_2$: a review. Int. J. Greenhouse Gas Control. 38, 26–43.

Cline, J.D., 1969. Spectrophotometric determination of hydrogen sulfide in natural waters. Limnol. Oceanogr. 14, 454–458.

Croudace, I.W., Williams-Thorpe, O., 1988. A low dilution, wavelength-dispersive x-ray fluoresence procedure for the analysis of aechaeological rock artefacts. Archaeometry 30, 227–236.

De Orte, M.R., Lombardi, A.T., Sarmiento, A.M., Basallote, M.D., Rodriguez-Romero, A., Riba, I., Valls, A.D., 2014. Metal mobility and toxicity to microalgae associated with acidification of sediments: CO_2 and acid comparison. Mar. Environ. Res. 96, 136–144.

Dickson, A.G., Millero, F.J., 1987. A comparison of the equilibrium constants for the dissociation of carbonic acid in seawater media. Deep Sea Res. A34 (10), 1733–1743.

Dickson, A.G., Sabine, C., Christian, J.R. (Eds.), 2007. Guide to Best Practices for Ocean CO_2 Measurements PICES Special Publication 3. North Pacific Marine Science Organization, Sidney, BC, Canada, p. 191.

Energy technology perspectives, 2008. International Energy Agency. Energy technology perspectives, Paris.

Duncan, I.J., Wang, H., 2014. Estimating the likelihood of pipeline failure in CO_2 transmission pipelines: new insights on risks of carbon capture and storage. Int. J. Greenhouse Gas Control 21, 49–60.

Fabricius, K.E., Langdon, C., Uthicke, S., Humphrey, C., Noonan, S., De/'ath, G., Okazaki, R., Muehllehner, N., Glas, M.S., Lough, J.M., 2011. Losers and winners in coral reefs acclimatized to elevated carbon dioxide concentrations. Nat. Clim. Change 1, 165–169.

Fisher, R., Lowry, D., Wilkin, O., Sriskantharajah, S., Nisbet, E.G., 2006. High-precision, automated stable isotope analysis of atmospheric methane and carbon dioxide using continuous-flow isotope-ratio mass spectrometry. Rapid Commun. Mass Spectrom. 20, 200–208.

Ganor, J., Mogollón, J.L., Lasaga, A.C., 1995. The effect of pH on kaolinite dissolution rates and on activation energy. Geochim. Cosmochim. Acta 59, 1037–1052.

Gherardi, F., Xu, T., Pruess, K., 2007. Numerical modeling of self-limiting and self-enhancing caprock alteration induced by CO_2 storage in a depleted gas reservoir. Chem. Geol. 244, 103–129.

Glover, A., 2009. Opportunities for CO_2 Storage Around Scotland—An Integrated Strategic Research Study. Scottish Government, pp. 56.

Gran, G., 1952. Determination of the equivalent point in potmeniometric titrations. Part II. Analyst 77, 661–671.

Gunter, W.D., Wong, S., Cheel, D.B., Sjostrom, G., 1998. Large CO_2 sinks: their role in the mitigation of greenhouse gases from an international, national (Canadian) and provincial (Alberta) perspective. Appl. Energy 61, 209–227.

Holloway, S., 2005. Underground sequestration of carbon dioxide—a viable greenhouse gas mitigation option. Energy 30, 2318–2333.

IEA Greenhouse Gas R&D programme (IEA GHG) Assessment of SubSea EcosystemImpacts, 2008/8, 577 August 2008.

Implementation of Directive 2009/31/EC on the Geological Storage of Carbon Dioxide, Guidance Document 1: CO_2 Storage Life Cycle Risk Management Framework European Communities, 2011, ISBN-13978-92-79-19833-5 doi: 10.2834/9801.

IPCC, 2005. (Intergovernmental Panel on Climate Change) Special Report on Carbon Dioxide Capture and Storage, Prepared by Working Group III of the Intergovernmental Panel on Climate Change. IPCC, Cambridge, MA, pp. 442.

IPCC, 2006. In: Eggleston, H.S., Buendia, L., Miwa, K., Ngara, T., Tanabe, K. (Eds.), IPCC (Intergovernmental Panel on Climate Change) Guidelines for National Greenhouse Gas Inventories, Prepared by the National Greenhouse Gas Inventories Programme. IGES, Japan, www.ipcc-nggip.iges.or.jp/public/2006gl.

Ishida, H., Golmen, L.G., West, J., Krüger, M., Coombs, P., Berge, J.A., Fukuhara, T., Magi, M., Kita, J., 2013. Effects of CO_2 on benthic biota: an in situ benthic chamber experiment in Storfjorden (Norway). Mar. Pollut. Bull. 73, 443–451.

Klump, V., Martens, C.S., 1989. The seasonality of nutrient regeneration in an organic-rich coastal sediment: kinetic modeling of changing pore-water nutrient and sulfate distributions. Limnol. Oceanogr. 34, 559–577.

Klusman, R.W., 2003. A geochemical perspective and assessment of leakage potential for a mature carbon dioxide-enhanced oil recovery project and as a prototype for carbon dioxide sequestration; Rangely field, Colorado. AAPG Bull. 87, 1485–1507.

Kirsch, K., Navarre-Sitchler, A.K., Wunsch, A., McCray, J.E., 2014. Metal release from sandstones under experimentally and numerically simulated CO_2 leakage conditions. Environ. Sci. Technol. 48, 1436–1442.

Kita, J., Stahl, H., Hyashi, M., Green, T., Watanabe, Y., Widdicombe, S., 2015. Benthic megafauna and CO_2 bubble dynamics observed by underwater photography during a controlled sub-seabed release of CO_2. Int. J. Greenhouse Gas Control. 38, 202–209.

Kovscek, A.R., 2002. Screening criteria for CO_2 storage in oil reservoirs. Pet. Sci. Technol. 20, 841–866.

Krause, E., Wichels, A., Giménez, L., Lunau, M., Schilhabel, M.B., Gerdts, G., 2012. Small changes in pH have direct effects on marine bacterial community composition: a microcosm approach. PLoS One 7 (10).

Kronimus, A., Busch, A., Alles, S., Juch, D., Jurisch, A., Littke, R., 2008. A preliminary evaluation of the CO_2 storage potential in unminable coal seams of the Münster Cretaceous Basin, Germany. Int. J. Greenhouse Gas Control 2, 329–341.

Long, E., Macdonald, D., Smith, S., Calder, F., 1995. Incidence of adverse biological effects within ranges of chemical concentrations in marine and estuarine sediments. Environ. Manage. 19, 81–97.

López, I., Kalman, J., Vale, C., Blasco, J., 2010. Influence of sediment acidification on the bioaccumulation of metals in Ruditapes philippinarum. Environ. Sci. Pollut. Res. 17, 1519–1528.

Mattey, D., Lowry, D., Duffet, J., Fisher, R., Hodge, E., Frisia, S., 2008. A 53 year seasonally resolved oxygen and carbon isotope record from a modern Gibraltar speleothem: reconstructed drip water and relationship to local precipitation. Earth Planet. Sci. Lett. 269, 80–95.

Mehrbach, C., Culberson, C.H., Hawly, J.H., Pytkowicz, R.M., 1973. Measurement of the apparent dissociation constants of carbonic acid in seawater at atmospheric pressure. Limnol. Oceanogr. 18, 897–907.

Mickler, P.J., Yang, C., Scanlon, B.R., Reedy, R., Lu, J., 2013. Potential impacts of CO_2 leakage on groundwater chemistry from laboratory batch experiments and field push–pull tests. Environ. Sci. Technol. 47, 10694–10702.

Murray, F., Widdicombe, S., McNeill, C.L., Solan, M., 2013. Consequences of a simulated rapid ocean acidification event for benthic ecosystem processes and functions. Mar. Pollut. Bull. 73, 435–442.

OSPAR, 2007. Guidelines for Risk Assessment and Management of Storage of CO_2 Streams in Geological Formations. OSPAR.

Payán, M.C., Verbinnen, B., Galan, B., Coz, A., Vandecasteele, C., Viguripavan, J.R., 2012. Potential influence of CO_2 release from a carbon capture storage site on release of trace metals from marine sediment. Environ. Pollut. 162, 29–39.

Pierrot, D., Lewis, E., Wallace, D.W.R., 2006. MS Excel Program Developed for CO2 System Calculations. Carbon Dioxide Information Analysis Eenter. Oak Ridge National Laboratory, U.S. Department of Energy, Oak Ridge, TN.

Riba, I., García-Luque, E., Blasco, J., DelValls, T.A., 2003. Bioavailability of heavy metals bound to estuarine sediments as a function of pH and salinity values. Chem. Speciation Bioavailability 15, 101–114.

Riebesell, U., Schulz, K.G., Bellerby, R.G.J., Botros, M., Fritsche, P., Meyerhofer, M., Neill, C., Nondal, G., Oschlies, A., Wohlers, J., Zollner, E., 2007. Enhanced biological carbon consumption in a high CO_2 ocean. Nature 450, 545–548.

Stevenson, A.G., 2001. Metal concentrations in marine sediments around Scotland: a baseline for environmental studies. Cont. Shelf Res. 21, 879–897.

Tait, K., Stahl, H., Taylor, P., Widdicombe, S., 2015. Rapid response of the active microbial community to CO_2 exposure from a controlled sub-seabed CO_2 leak in Ardmucknish Bay (Oban), Scotland. Int. J. Greenhouse Gas Control. 38, 171–181.

Taylor, P., Lichtschlag, A., Tobermann, M., Sayer, M.D.J., Reynolds, A., Sato, T., and Stahl, H., 2014a. Impact and recovery of pH in marine sediments subject to a temporary carbon dioxide leak. Int. J. Greenhouse Gas Control.

Taylor, P., Stahl, H., Blackford, J., Vardy, M.E., Bull, J., Ackhurst, M., Hauton, C., James, R., Lichtschlag, A., Long, D., Montgomery, J., Naylor, M., Connelly, D., Smith, D., Sayer, M.D.J., Widdicombe, S., Wright, I.C., 2015-b. A novel sub-seabed CO_2 release experiment informing monitoring and impact assessment for geological carbon storage. Int. J. Greenhouse Gas Control 38, 3–17.

Turekian, K.K., 1968. Oceans. Prentice-Hall, pp. 120.

Vangkilde-Pedersen, T., Anthonsen, K.L., Smith, N., Kirk, K., Neele, F., van der Meer, B., Le Gallo, Y., Bossie-Codreanu, D., Wojcicki, A., Le Nindre, Y.-M., Hendriks, C., Dalhoff, F., Peter Christensen, N., 2009. Assessing European capacity for geological storage of carbon dioxide—the EU GeoCapacity project. Energy Procedia 1, 2663–2670.

White, C.M., Smith, D.H., Jones, K.L., Goodman, A.L., Jikich, S.A., LaCount, R.B., DuBose, S.B., Ozdemir, E., Morsi, B.I., Schroeder, K.T., 2005. Sequestration of carbon dioxide in coal with enhanced coalbed methane recovery. Energy Fuels 19, 659–724.

Widdicombe, S., Smith, D.H., Mcneill, C.L., Stahl, H., Taylor, P., Queiros, A.M., Nunes, J., Tait, K., 2015. Impact of sub-seabed CO_2 leakage on macrobenthic community structure and diversity. Int. J. Greenhouse Gas Control 38, 182–192.

Winkler, L., 1888. The determination of dissolved oxygen in water. Bericht der Deutschen Chemischen Gesellschaft, 21., pp. 2843–2857.

Wunsch, A., Navarre-Sitchler, A.K., Moore, J., McCray, J.E., 2014. Metal release from limestones at high partial-pressures of CO_2. Chem. Geol. 363, 40–55.

Wunsch, A., Navarre-Sitchler, A.K., Moore, J., Ricko, A., McCray, J.E., 2013. Metal release from dolomites at high partial-pressures of CO_2. Appl. Geochem. 38, 33–47.

Zeebe, R.E., Gladrow, W.-D., 2001. CO_2 in Seawater: Equilibrium, Kinetics and Isotopes. Elsevier Science, B.V., Amsterdam.

Zhang, L., Ren, S., Ren, B., Zhang, W., Guo, Q., Zhang, L., 2011. Assessment of CO_2 storage capacity in oil reservoirs associated with large lateral/underlying aquifers: case studies from China. Int. J. Greenhouse Gas Control 5, 1016–1021.